

A NOVEL PERSPECTIVE FOR SOLUTIONS OF THE GARDNER EQUATION USING TWO RELIABLE METHODS

DERYA YILDIRIM SUCU¹, KHALİD K. ALİ², MÜJDET GÜNGÖR¹,
SEYDİ BATTAL GAZİ KARAKOC¹

Manuscript received: 25.03.2025; Accepted paper: 06.09.2025;

Published online: 30.09.2025.

Abstract. The main goal of this article is to find different and new analytical and numerical solutions of the Gardner equation. The equation, also known as the combined KdV–mKdV equation, clarifies several interesting physical phenomena, such as internal waves in a stratified ocean [1], long wave propagation in an inhomogeneous two-layer shallow liquid [2], and ion acoustic waves in plasma with negative ions [3]. Our study consists of two main parts: in the first part, (G'/G) – expansion method is implemented to create some alternative exact solutions of the Gardner equation. Also in this part, various hypotheses are considered to construct many exact traveling wave solutions (involving Hyperbolic, Trigonometric, and Rational solutions). In the second part, a collocation method based on the septic B-spline approximation has been introduced and put into practice for the numerical solution of the equation while taking various test problem parameter values into account. Additionally, Von-Neumann stability analysis has been carried out, ensuring the scheme's unconditional stability. The appropriate solutions for the two test problems are found by computing the L_2 and L_∞ error norms, which highlight the significance of the procedure and demonstrate its applicability and credibility. The numerical findings are inferred to match the analytical answers well, suggesting that the existing B-spline collocation algorithm is strong and appealing. The results are tabulated and reported both modally and in terms of the productivity of the procedure. The results produced from both analytical and numerical methods demonstrate the great utility of this study for scientists tasked with identifying characteristics and features of nonlinear processes across a variety of scientific domains.

Keywords: Gardner equation; (G'/G) – expansion method; collocation; septic B-spline.

1. INTRODUCTION

As it is known, nonlinear evolution equations (NLEEs) have been generally considered to characterise physical properties in a large area of scientific and engineering fields, including applied mathematics, mathematical biology, mathematical physics, theory of solitons, hydrodynamics, optical fibres, marine engineering, plasma physics, fluid mechanics and chaos theory to investigate propagation of the waves [4]. As it can ensure many physical features and more awareness of the physical perspectives of the problems and thus contribute to further applications, examination of the traveling wave solutions for NLEEs play a vital role in nonlinear science fields [5-7].

¹ Nevşehir Hacı Bektaş Veli University, Faculty of Sciences and Arts, Department of Mathematics, 50300 Turkey.
E-mail: dryldrmsucu@gmail.com; mujdetgungor@nevsehir.edu.tr; sbgkarakoc@nevsehir.edu.tr.

² Al-Azhar University, Faculty of Sciences, Department of Mathematics, Nasr-City, Cairo, Egypt.
E-mail: khalidkaram2012@azhar.edu.eg.

Therefore, it is significant to concentrate on solitary waves and search for exact traveling wave solutions in a detailed manner from a mathematical point of view. Up to now, many robust methods to construct exact solutions of NLEEs have been created and developed. Among others, Hirota bilinear method [8,9], Backlund transformations method [10], Kudryashov method [11], generalized Kudryashov method [12,13], modified exponential function method [14], inverse scattering method [15], F-expansion method [16], the sine-cosine and tanh methods [17], Exp-function method [18,19], (G'/G) – expansion method [20-23], Jacobi elliptic functions method [24,25], Sinc-Galerkin method [26], bilinear transformation method [27,28], Riccati equation method [29], and so on. The above methods have derived many types of solutions from most NLEEs. In this study, we have offered the following well-known NLEE, namely the Gardner equation:

$$u_t + (au + \gamma u^2)u_x + \beta u_{xxx} = 0, \quad (1)$$

where the coefficients in the equation are all constants. Equation (1) becomes a very attractive equation for nonlinear wave propagation because of the struggle between the nonlinear terms and the third-order dispersive term. Solutions of Equation (1) depend cardinally on the sign of the coefficient of the cubic non-linear term γ . In particular, if $\gamma < 0$ there is one family of solitary waves (solitons) only, if $\gamma > 0$ there are two families of solitons, and also breathers (oscillating wave packets) exist. The Gardner equation is completely integrable, as for the following Korteweg-de Vries (KdV) equation,

$$u_t + auu_x + \beta u_{xxx} = 0, \quad (2)$$

and first arose in the derivation of the infinite number of conservation laws for the KdV equation [30]. The Gardner equation has been used to model rogue waves in layered fluids, such as in the atmosphere and river mouths, including both solitons and undular bore solutions [31,32]. One of the best-known applications of this equation is the modeling of large-amplitude internal waves [33-35]. Much attention has been paid to the Gardner equation [36-56], but looking for more interesting new solutions still remains a major contribution. Besides, the numerical behavior of the equation has also been of interest in the literature [57-59]. In this study, we applied effective and powerful methods to obtain the exact and numerical solutions of the Gardner equation, which has been studied extensively. Thus, the sections of the paper are arranged as follows: We begin in Section 2 with the mathematical analysis of the model. Strategy of the (G'/G) – expansion method is analyzed in Section 3. In Section 4, (G'/G) – expansion method is used to obtain a new family of analytical solutions of the equation. Section 5 discusses the graphical representation of several of these solutions. Section 6 shows how to apply the collocation approach to the equation. The scheme's stability analysis is the main topic of Section 7. We conduct comprehensive numerical testing of our suggested scheme in Section 8 to examine the sensitivity and capabilities of our model, and we conclude with general findings in Section 9.

2. MAIN IDEA OF THE METHOD

To procure a traveling wave solution of the Equation (1) and the following equation, which is a special case of Equation (1),

$$u_t + u_{xxx} + 6u^2u_x + 6uu_x = 0, \quad (3)$$

we utilize the subsequent transformation:

$$u(x, t) = v(\eta) \quad (4)$$

where

$$\eta = kx - \vartheta t \quad (5)$$

and ϑ represents the traveling wave's speed. We can rewrite Equations (1) and (3) as follows by using Equations (4) and (5):

$$k^3 v^3(\eta) + v'(\eta)(6kv(\eta)(v(\eta) + 1) - \vartheta) = 0, \quad (6)$$

$$v^3 v^{(3)}(\eta) = 0. \quad (7)$$

Then, we can solve (6) and (7) to find the solutions of the Equations (1) and (3).

3. THE (G'/G) – EXPANSION TECHNIQUE'S METHODOLOGY

The following is how one can formulate the governing equation:

$$F(u, u_{xx}, u_{tt}, \dots) = 0. \quad (8)$$

A polynomial function F in Equation (8) is dependent on the function u and its derivatives in space and time. We may use a traveling wave transformation (4) with (5) to translate this partial differential equation (PDE) into an ordinary differential equation (ODE):

$$H(v, v''', \dots) = 0. \quad (9)$$

The principal steps of the (G'/G) – expansion method are as follows [60]:

Step 1. First, we will assume that the exact solutions to Equation (9)

$$v(\eta) = \sum_{i=0}^N R_i \left(\frac{G'}{G} \right)^i, \quad (10)$$

where $G = G(\eta)$ guarantees the second-order linear ODE written by:

$$G''(\eta) + \sigma G'(\eta) + vG(\eta) = 0, \quad (11)$$

where the constants $R_i (i = 0, 1, 2, \dots, N)$, $R_N \neq 0$, σ and v need to be computed.

Step 2. There is a highest power nonlinear term and a highest order derivative term in Equation (9). By balancing these two terms, a positive integer N is obtained, as shown in Equation (10). This integer value is likely to be significant in characterizing the behavior of the system described by the equations, although further information about the equations are necessary to fully understand the meaning of N .

Step 3. Equation (11) has three different families of traveling wave solutions that we can identify:

Family 1: solutions for hyperbolic functions, when, $\sigma^2 - 4v > 0$,

$$\frac{G'}{G} = \frac{-\sigma}{2} + \frac{1}{2}\sqrt{\sigma^2 - 4v} \frac{g_1 \sinh \frac{1}{2}\sqrt{\sigma^2 - 4v}\eta + g_2 \cosh \frac{1}{2}\sqrt{\sigma^2 - 4v}\eta}{g_1 \cosh \frac{1}{2}\sqrt{\sigma^2 - 4v}\eta + g_2 \sinh \frac{1}{2}\sqrt{\sigma^2 - 4v}\eta} \quad (12)$$

Family 2: solutions for trigonometric functions, when $\sigma^2 - 4v < 0$,

$$\frac{G'}{G} = \frac{-\sigma}{2} + \frac{1}{2}\sqrt{4v - \sigma^2} \frac{-g_1 \sinh \frac{1}{2}\sqrt{4v - \sigma^2}\eta + g_2 \cosh \frac{1}{2}\sqrt{4v - \sigma^2}\eta}{g_1 \cosh \frac{1}{2}\sqrt{4v - \sigma^2}\eta + g_2 \sinh \frac{1}{2}\sqrt{4v - \sigma^2}\eta}. \quad (13)$$

Family 3: solutions for rational functions, when $\sigma^2 - 4v = 0$

$$\frac{G'}{G} = \frac{-\sigma}{2} + \frac{g_2}{g_1 + g_2\eta}. \quad (14)$$

Step 4. By substituting Equation (10) for Equation (9) and using Equation (11) to arrange the terms with identical powers of $\left(\frac{G'}{G}\right)$ together, we may construct a system of algebraic equations in R_i, k , and ϑ . We then equate each coefficient to zero, and this system of equations can be solved using the Mathematica program.

4. NEW SOLUTION FAMILIES OBTAINED FOR THE (G'/G) - EXPANSION METHOD

In this part, we provide analytical solutions for two cases studied in problem (1) using the (G'/G) - expansion method. For the purpose of approximating solutions to nonlinear differential equations, the (G'/G) - expansion approach is an exceptional analytical tool.

4.1. THE FIRST MODEL'S ANALYTICAL SOLUTIONS

Applying the balance principle to (6) between the terms v^2v' and $v^{(3)}$ yields $3N + 1 = N + 3$, which implies that $N = 1$. Using (10), we can express the solution of (6) as follows:

$$v(\eta) = \sum_{i=0}^1 R_i \left(\frac{G'}{G}\right)^i. \quad (15)$$

If equality (15) is written in Equation (6) and even up the coefficients of like powers of $\left(\frac{G'}{G}\right)$ to zero, the following system is obtained:

$$\begin{aligned} -2k^3v^2R_1 - k^3vR_1\sigma^2 - 6kvR_0^2R_1 - 6kvR_0R_1 + vR_1\vartheta &= 0, \\ -8k^3vR_1\sigma + k^3R_1(-\sigma^3) - 6kvR_1^2 - 12kvR_0R_1^2 - 6kR_0^2R_1\sigma - 6kR_0R_1\sigma + R_1\sigma + \vartheta &= 0, \\ -8k^3vR_1 - 7k^3R_1\sigma^2 - 6kvR_1^3 - 6kR_1^2\sigma - 12kR_0R_1^2\sigma - 6kR_0^2R_1 - 6kR_0R_1 + R_1 + \vartheta &= 0, \end{aligned}$$

$$\begin{aligned} -12k^3R_1\sigma - 6kR_1^3\sigma - 12kvR_0R_1^2 - 6kR_1^2 &= 0, \\ -6k^3R_1 - 6kR_1^3 &= 0. \end{aligned}$$

By solving the system of equations given above R_0 , R_1 and k are obtained as:

$$\begin{aligned} R_0 &= \frac{1}{2} \left(\mp \sqrt{\frac{\sigma^2 \left(4v - \sigma^2 + \left(\sqrt{(4v - \sigma^2)^3 (\vartheta^2(4v - \sigma^2) - 1)} - \vartheta(\sigma^2 - 4v)^2 \right)^{2/3} \right)^2}{(\sigma^2 - 4v)^2 \left(\sqrt{(4v - \sigma^2)^3 (\vartheta^2(4v - \sigma^2) - 1)} - \vartheta(\sigma^2 - 4v)^2 \right)^{2/3}}} - 1 \right), \\ R_1 &= \mp \sqrt{\frac{\sigma^2 \left(4v - \sigma^2 + \left(\sqrt{(4v - \sigma^2)^3 (\vartheta^2(4v - \sigma^2) - 1)} - \vartheta(\sigma^2 - 4v)^2 \right)^{2/3} \right)^2}{(\sigma^2 - 4v)^2 \left(\sqrt{(4v - \sigma^2)^3 (\vartheta^2(4v - \sigma^2) - 1)} - \vartheta(\sigma^2 - 4v)^2 \right)^{2/3}}}, \\ k &= \frac{-4v + \sigma^2 - \left(\sqrt{(4v - \sigma^2)^3 (\vartheta^2(4v - \sigma^2) - 1)} - \vartheta(\sigma^2 - 4v)^2 \right)^{2/3}}{(4v - \sigma^2)^3 \sqrt{\sqrt{(4v - \sigma^2)^3 (\vartheta^2(4v - \sigma^2) - 1)} - \vartheta(\sigma^2 - 4v)^2}}. \end{aligned} \quad (16)$$

When equalities (16), (15) and (5) with Equation (4) are used in Equation (1) solutions of Equation (1) have been procured as follows:

Family 1: solutions for hyperbolic functions, when $\sigma^2 - 4v > 0$,

$$\begin{aligned} u_{1,2}(x, t) &= \frac{1}{2} \ln \left(R_0 \right. \\ &\quad + R_1 \left(\frac{-\sigma}{2} + \frac{1}{2} \sqrt{\sigma^2 - 4v} \frac{g_1 \sinh \frac{1}{2} \sqrt{\sigma^2 - 4v} \eta + g_2 \cosh \frac{1}{2} \sqrt{\sigma^2 - 4v} \eta}{g_1 \cosh \frac{1}{2} \sqrt{\sigma^2 - 4v} \eta + g_2 \sinh \frac{1}{2} \sqrt{\sigma^2 - 4v} \eta} \right) \\ &\quad \left. + R_2 \left(\frac{-\sigma}{2} + \frac{1}{2} \sqrt{\sigma^2 - 4v} \frac{g_1 \sinh \frac{1}{2} \sqrt{\sigma^2 - 4v} \eta + g_2 \cosh \frac{1}{2} \sqrt{\sigma^2 - 4v} \eta}{g_1 \cosh \frac{1}{2} \sqrt{\sigma^2 - 4v} \eta + g_2 \sinh \frac{1}{2} \sqrt{\sigma^2 - 4v} \eta} \right)^2 \right). \end{aligned} \quad (17)$$

Family 2: solutions for trigonometric functions, when $\sigma^2 - 4v < 0$,

$$\begin{aligned}
u_{3,4}(x, t) = & \frac{1}{2} \ln \left(R_0 \right. \\
& + R_1 \left(\frac{-\sigma}{2} + \frac{1}{2} \sqrt{\sigma^2 - 4v} \frac{-g_1 \sin \frac{1}{2} \sqrt{\sigma^2 - 4v} \eta + g_2 \cos \frac{1}{2} \sqrt{\sigma^2 - 4v} \eta}{g_1 \cos \frac{1}{2} \sqrt{\sigma^2 - 4v} \eta + g_2 \sin \frac{1}{2} \sqrt{\sigma^2 - 4v} \eta} \right) \\
& + R_2 \left(\frac{-\sigma}{2} \right. \\
& \left. \left. + \frac{1}{2} \sqrt{\sigma^2 - 4v} \frac{-g_1 \sin \frac{1}{2} \sqrt{\sigma^2 - 4v} \eta + g_2 \cos \frac{1}{2} \sqrt{\sigma^2 - 4v} \eta}{g_1 \cos \frac{1}{2} \sqrt{\sigma^2 - 4v} \eta + g_2 \sin \frac{1}{2} \sqrt{\sigma^2 - 4v} \eta} \right)^2 \right). \quad (18)
\end{aligned}$$

4.2. THE SECOND MODEL'S ANALYTICAL SOLUTIONS

By considering the balance principle to Equation (15) between the terms v'^2 and $v^{(3)}$, we arrive at $3N + 1 = N + 3$, which implies that $N = 1$. Using (10), we can express the solution to (7) as follows:

From (10), the solution of (7) can be presented as:

$$f(\eta) = \sum_{i=0}^1 R_i \left(\frac{G'}{G} \right)^i. \quad (19)$$

By substituting Equation (19) into Equation (7) and equating the coefficients of like powers of $\left(\frac{G'}{G} \right)$ to zero, we obtain the following system:

$$\begin{aligned}
-8CR_0^2 + k^2 v^2 R_1^2 + 8qR_0^3 - v^2 R_1^2 \vartheta^2 - 2R_0^4 &= 0, \\
-16CR_0 R_1 + 2k^2 v R_1^2 \sigma + 24qR_1 R_0^2 - 2v R_1^2 \sigma \vartheta^2 - 8R_1 R_0^3 &= 0, \\
-8CR_1^2 + 2k^2 v R_1^2 + k^2 R_1^2 \sigma^2 + 24qR_0 R_1^2 - 2v R_1^2 \vartheta^2 - R_1^2 \sigma^2 \vartheta^2 - 12R_0^2 R_1^2 &= 0, \\
2k^2 R_1^2 \sigma + 8qR_1^3 - 2R_1^2 \sigma \vartheta^2 - 8R_0 R_1^3 &= 0, \\
2k^2 R_1^2 - R_1^2 \vartheta^2 - 2R_1^4 &= 0.
\end{aligned}$$

The following sets of solutions were obtained by using the Mathematica program to solve the previously described set of equations:

• **Set 1:**

$$R_0 = 0, \quad k = \mp \frac{\sqrt[3]{-1} \sqrt[3]{\vartheta}}{\sqrt[3]{2cv + c\sigma^2}}, \quad a = \mp \frac{6(-1)^{2/3} c \sigma \vartheta^{2/3}}{R_1 (c(2v + \sigma^2))^{2/3}}, \quad b = \mp \frac{6(-1)^{2/3} c \vartheta^{2/3}}{R_1^2 (c(2v + \sigma^2))^{2/3}}. \quad (20)$$

Substituting from (17) to (19) with (4), (5) respectively, we get the solutions of (3):

Family 1: solutions for hyperbolic functions, when $\sigma^2 - 4v > 0$,

$$\begin{aligned}
u_{1,2}(x,t) = \ln & \left(R_0 \right. \\
& + R_1 \left(\frac{-\sigma}{2} + \frac{1}{2} \sqrt{\sigma^2 - 4v} \frac{g_1 \sinh \frac{1}{2} \sqrt{\sigma^2 - 4v} \eta + g_2 \cosh \frac{1}{2} \sqrt{\sigma^2 - 4v} \eta}{g_1 \cosh \frac{1}{2} \sqrt{\sigma^2 - 4v} \eta + g_2 \sinh \frac{1}{2} \sqrt{\sigma^2 - 4v} \eta} \right) \\
& \left. + R_2 \left(\frac{-\sigma}{2} + \frac{1}{2} \sqrt{\sigma^2 - 4v} \frac{g_1 \sinh \frac{1}{2} \sqrt{\sigma^2 - 4v} \eta + g_2 \cosh \frac{1}{2} \sqrt{\sigma^2 - 4v} \eta}{g_1 \cosh \frac{1}{2} \sqrt{\sigma^2 - 4v} \eta + g_2 \sinh \frac{1}{2} \sqrt{\sigma^2 - 4v} \eta} \right)^2 \right)^{\frac{1}{2}}. \quad (21)
\end{aligned}$$

Family 2: solutions for trigonometric functions, when $\sigma^2 - 4v < 0$,

$$\begin{aligned}
u_{3,4}(x,t) = \ln & \left(R_0 \right. \\
& + R_1 \left(\frac{-\sigma}{2} + \frac{1}{2} \sqrt{\sigma^2 - 4v} \frac{-g_1 \sin \frac{1}{2} \sqrt{\sigma^2 - 4v} \eta + g_2 \cos \frac{1}{2} \sqrt{\sigma^2 - 4v} \eta}{g_1 \cos \frac{1}{2} \sqrt{\sigma^2 - 4v} \eta + g_2 \sin \frac{1}{2} \sqrt{\sigma^2 - 4v} \eta} \right) \\
& \left. + R_2 \left(\frac{-\sigma}{2} + \frac{1}{2} \sqrt{\sigma^2 - 4v} \frac{-g_1 \sin \frac{1}{2} \sqrt{\sigma^2 - 4v} \eta + g_2 \cos \frac{1}{2} \sqrt{\sigma^2 - 4v} \eta}{g_1 \cos \frac{1}{2} \sqrt{\sigma^2 - 4v} \eta + g_2 \sin \frac{1}{2} \sqrt{\sigma^2 - 4v} \eta} \right)^2 \right)^{\frac{1}{2}}. \quad (22)
\end{aligned}$$

• **Set 2:**

$$R_1 = \frac{R_0}{\sigma}, k = \mp \frac{\sqrt[3]{-1} \sqrt[3]{\vartheta}}{\sqrt[3]{2cv + c\sigma^2}}, a = \mp \frac{6(-1)^{2/3} c \sigma^2 \vartheta^{2/3}}{R_0 (c(2v + \sigma^2))^{2/3}}, b = \mp \frac{6(-1)^{2/3} c \sigma^2 \vartheta^{2/3}}{R_0^2 (c(2v + \sigma^2))^{2/3}}. \quad (23)$$

Substituting from (17) to (19) with (4), (5) respectively, we get the solutions of (3):

Family 1: solutions for hyperbolic functions, when $\sigma^2 - 4v > 0$,

$$\begin{aligned}
u_{5,6}(x,t) = \ln & \left(R_0 \right. \\
& + R_1 \left(\frac{-\sigma}{2} + \frac{1}{2} \sqrt{\sigma^2 - 4v} \frac{g_1 \sinh \frac{1}{2} \sqrt{\sigma^2 - 4v} \eta + g_2 \cosh \frac{1}{2} \sqrt{\sigma^2 - 4v} \eta}{g_1 \cosh \frac{1}{2} \sqrt{\sigma^2 - 4v} \eta + g_2 \sinh \frac{1}{2} \sqrt{\sigma^2 - 4v} \eta} \right) \\
& \left. + R_2 \left(\frac{-\sigma}{2} + \frac{1}{2} \sqrt{\sigma^2 - 4v} \frac{g_1 \sinh \frac{1}{2} \sqrt{\sigma^2 - 4v} \eta + g_2 \cosh \frac{1}{2} \sqrt{\sigma^2 - 4v} \eta}{g_1 \cosh \frac{1}{2} \sqrt{\sigma^2 - 4v} \eta + g_2 \sinh \frac{1}{2} \sqrt{\sigma^2 - 4v} \eta} \right)^2 \right)^{\frac{1}{2}}. \quad (24)
\end{aligned}$$

Family 2: solutions for trigonometric functions, when $\sigma^2 - 4v < 0$,

$$\begin{aligned}
u_{7,8}(x, t) = \ln \left(R_0 \right. \\
+ R_1 \left(\frac{-\sigma}{2} + \frac{1}{2} \sqrt{\sigma^2 - 4v} \frac{-g_1 \sin \frac{1}{2} \sqrt{\sigma^2 - 4v} \eta + g_2 \cos \frac{1}{2} \sqrt{\sigma^2 - 4v} \eta}{g_1 \cos \frac{1}{2} \sqrt{\sigma^2 - 4v} \eta + g_2 \sin \frac{1}{2} \sqrt{\sigma^2 - 4v} \eta} \right) \\
\left. + R_2 \left(\frac{-\sigma}{2} + \frac{1}{2} \sqrt{\sigma^2 - 4v} \frac{-g_1 \sin \frac{1}{2} \sqrt{\sigma^2 - 4v} \eta + g_2 \cos \frac{1}{2} \sqrt{\sigma^2 - 4v} \eta}{g_1 \cos \frac{1}{2} \sqrt{\sigma^2 - 4v} \eta + g_2 \sin \frac{1}{2} \sqrt{\sigma^2 - 4v} \eta} \right)^2 \right)^{\frac{1}{2}}. \quad (25)
\end{aligned}$$

• Set 3:

$$R_1 = \frac{R_0}{\sigma}, k = \frac{\sqrt[3]{\vartheta}}{\sqrt[3]{2cv + c\sigma^2}}, a = \frac{6c\sigma^2\vartheta^{2/3}}{R_0(c(2v + \sigma^2))^{2/3}}, b = -\frac{6c\sigma^2\vartheta^{2/3}}{R_0^2(c(2v + \sigma^2))^{2/3}}. \quad (26)$$

Substituting from (17) to (19) with (4), (5) respectively, we get the solutions of (3):

Family 1: solutions for hyperbolic functions, when $\sigma^2 - 4v > 0$,

$$\begin{aligned}
u_9(x, t) = \ln \left(R_0 \right. \\
+ R_1 \left(\frac{-\sigma}{2} + \frac{1}{2} \sqrt{\sigma^2 - 4v} \frac{g_1 \sinh \frac{1}{2} \sqrt{\sigma^2 - 4v} \eta + g_2 \cosh \frac{1}{2} \sqrt{\sigma^2 - 4v} \eta}{g_1 \cosh \frac{1}{2} \sqrt{\sigma^2 - 4v} \eta + g_2 \sinh \frac{1}{2} \sqrt{\sigma^2 - 4v} \eta} \right) \\
\left. + R_2 \left(\frac{-\sigma}{2} + \frac{1}{2} \sqrt{\sigma^2 - 4v} \frac{g_1 \sinh \frac{1}{2} \sqrt{\sigma^2 - 4v} \eta + g_2 \cosh \frac{1}{2} \sqrt{\sigma^2 - 4v} \eta}{g_1 \cosh \frac{1}{2} \sqrt{\sigma^2 - 4v} \eta + g_2 \sinh \frac{1}{2} \sqrt{\sigma^2 - 4v} \eta} \right)^2 \right)^{\frac{1}{2}}. \quad (27)
\end{aligned}$$

Family 2: solutions for trigonometric functions, when $\sigma^2 - 4v < 0$

$$\begin{aligned}
u_{10}(x, t) = \ln \left(R_0 \right. \\
+ R_1 \left(\frac{-\sigma}{2} + \frac{1}{2} \sqrt{\sigma^2 - 4v} \frac{-g_1 \sin \frac{1}{2} \sqrt{\sigma^2 - 4v} \eta + g_2 \cos \frac{1}{2} \sqrt{\sigma^2 - 4v} \eta}{g_1 \cos \frac{1}{2} \sqrt{\sigma^2 - 4v} \eta + g_2 \sin \frac{1}{2} \sqrt{\sigma^2 - 4v} \eta} \right) \\
\left. + R_2 \left(\frac{-\sigma}{2} + \frac{1}{2} \sqrt{\sigma^2 - 4v} \frac{-g_1 \sin \frac{1}{2} \sqrt{\sigma^2 - 4v} \eta + g_2 \cos \frac{1}{2} \sqrt{\sigma^2 - 4v} \eta}{g_1 \cos \frac{1}{2} \sqrt{\sigma^2 - 4v} \eta + g_2 \sin \frac{1}{2} \sqrt{\sigma^2 - 4v} \eta} \right)^2 \right)^{\frac{1}{2}}. \quad (28)
\end{aligned}$$

• Set 4:

$$R_0 = 0, k = \frac{\sqrt[3]{\vartheta}}{\sqrt[3]{2cv + c\sigma^2}}, a = -\frac{6c\sigma^2\vartheta^{2/3}}{R_1(c(2v + \sigma^2))^{2/3}}, b = -\frac{6c\sigma^2\vartheta^{2/3}}{R_1^2(c(2v + \sigma^2))^{2/3}}. \quad (29)$$

Substituting from (17) to (19) with (4), (5) respectively, we get the solutions of (3):

Family 1: solutions for hyperbolic functions, when $\sigma^2 - 4v > 0$,

$$u_{11}(x, t) = \ln \left(R_0 + R_1 \left(\frac{-\sigma}{2} + \frac{1}{2} \sqrt{\sigma^2 - 4v} \frac{g_1 \sinh \frac{1}{2} \sqrt{\sigma^2 - 4v} \eta + g_2 \cosh \frac{1}{2} \sqrt{\sigma^2 - 4v} \eta}{g_1 \cosh \frac{1}{2} \sqrt{\sigma^2 - 4v} \eta + g_2 \sinh \frac{1}{2} \sqrt{\sigma^2 - 4v} \eta} \right) + R_2 \left(\frac{-\sigma}{2} + \frac{1}{2} \sqrt{\sigma^2 - 4v} \frac{g_1 \sinh \frac{1}{2} \sqrt{\sigma^2 - 4v} \eta + g_2 \cosh \frac{1}{2} \sqrt{\sigma^2 - 4v} \eta}{g_1 \cosh \frac{1}{2} \sqrt{\sigma^2 - 4v} \eta + g_2 \sinh \frac{1}{2} \sqrt{\sigma^2 - 4v} \eta} \right)^2 \right)^{\frac{1}{2}}. \quad (30)$$

Family 2: solutions for trigonometric functions, when $\sigma^2 - 4v < 0$

$$u_{12}(x, t) = \ln \left(R_0 + R_1 \left(\frac{-\sigma}{2} + \frac{1}{2} \sqrt{\sigma^2 - 4v} \frac{-g_1 \sin \frac{1}{2} \sqrt{\sigma^2 - 4v} \eta + g_2 \cos \frac{1}{2} \sqrt{\sigma^2 - 4v} \eta}{g_1 \cos \frac{1}{2} \sqrt{\sigma^2 - 4v} \eta + g_2 \sin \frac{1}{2} \sqrt{\sigma^2 - 4v} \eta} \right) + R_2 \left(\frac{-\sigma}{2} + \frac{1}{2} \sqrt{\sigma^2 - 4v} \frac{-g_1 \sin \frac{1}{2} \sqrt{\sigma^2 - 4v} \eta + g_2 \cos \frac{1}{2} \sqrt{\sigma^2 - 4v} \eta}{g_1 \cos \frac{1}{2} \sqrt{\sigma^2 - 4v} \eta + g_2 \sin \frac{1}{2} \sqrt{\sigma^2 - 4v} \eta} \right)^2 \right)^{\frac{1}{2}}. \quad (31)$$

5. GRAPHICAL ILLUSTRATIONS

We utilize the analytical approach in this part to explore the equation that we created. Two- and three-dimensional graphs of some of the analytical solutions were drawn to show the effectiveness and reliability of the obtained results. In Figs. 1-5, graphs of the analytical solutions of Equations (17), (22), (25), (27), and (30) using various parameter configurations are shown, respectively. These graphs provide insight into how the system's dynamics and the parameters employed affect the solutions' overall behavior. The results show valuable insights into the features and behavior of the solutions.

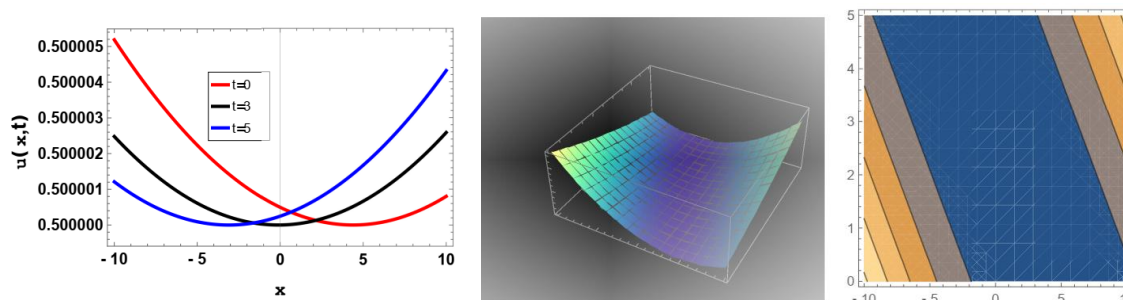


Figure 1. Graph of (17) at $g_2 = 0.05$, $g_1 = 0.9$, $v = 0.001$, $\sigma = 0.2$, $\vartheta = 0.2$.

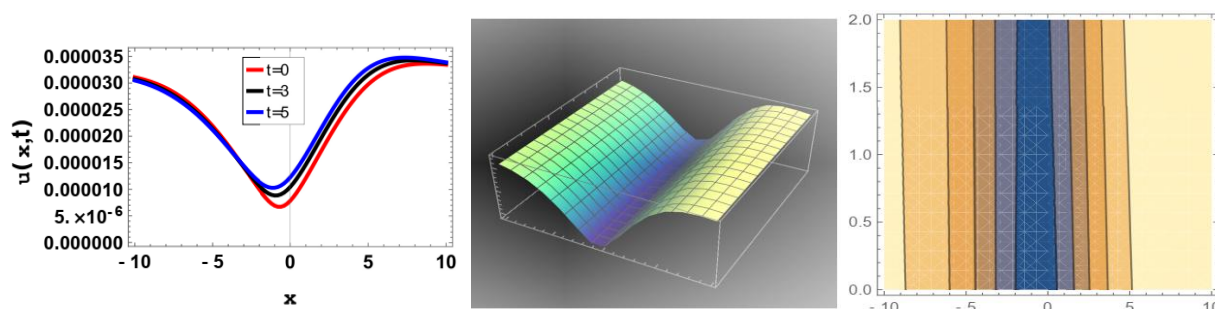


Figure 2. Graph of (22) at $g_2 = 0.2, c = 2, g_1 = 0.8, v = 0.001, R_1 = 0.001, \sigma = 0.0001, \vartheta = 0.8$.

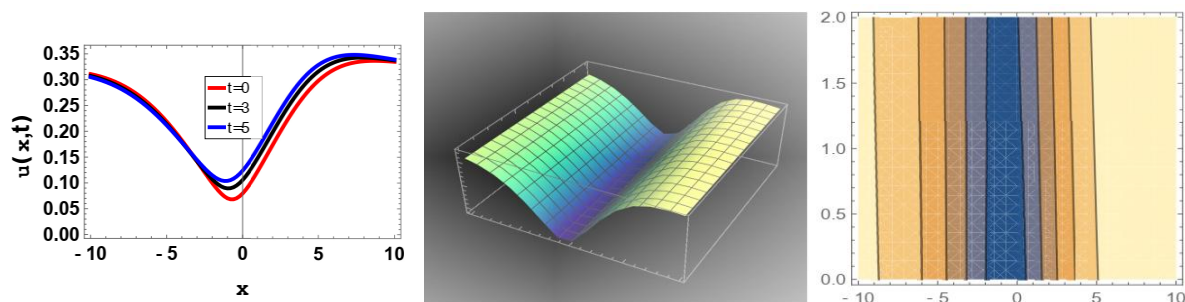


Figure 3. Graph of (25) at $g_2 = 0.2, c = 2, g_1 = 0.8, v = 0.001, R_0 = 0.001, \sigma = 0.0001, \vartheta = 0.8$.

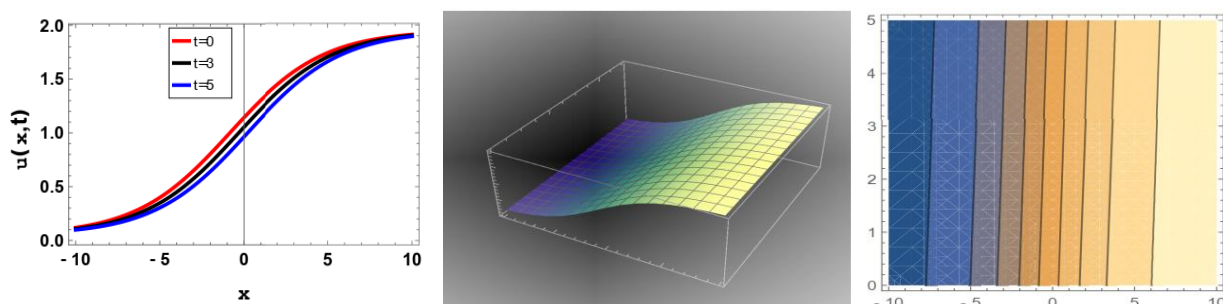


Figure 4. Graph of (27) at $g_2 = 0.3, c = 0.7, g_1 = 2, v = 0.001, R_0 = 2, \sigma = 0.2, \vartheta = 0.2$.

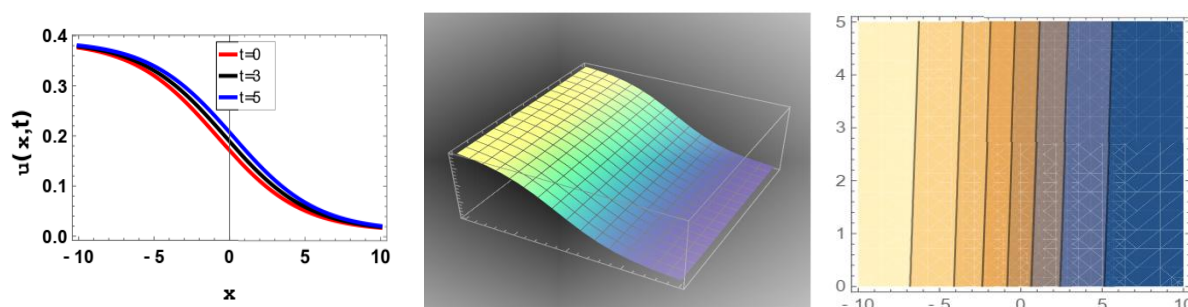


Figure 5. Graph of (30) at $g_2 = 0.3, c = 0.7, g_1 = 2, v = 0.001, R_1 = 2, \sigma = 0.2, \vartheta = 0.2$.

6. APPLICATION OF SEPTIC B-SPLINE COLLOCATION METHOD

This section deals with the mathematical issue represented by Equation (1) when certain septic B-splines are present. The definition of septic B-splines is found in [61], and they are important to this strategy. Among many numerical methods, the collocation method is a

method that gives good results and is very convenient in terms of time and workload [62]. In this method, $u_{numeric}(x, t)$ conforming with the $u_{exact}(x, t)$ can be written as follows:

$$u_{numeric}(x, t) = \sum_{m=-3}^{N+3} \phi_m(x) \sigma_m(t). \quad (32)$$

If $h\zeta = x - x_m$, $0 \leq \zeta \leq 1$, transformation is done in the range $[x_m, x_{m+1}]$, the range $[0, 1]$ is obtained. Thus, in the new range $[0, 1]$, septic B-spline functions are obtained in the manner described below [63]:

$$\begin{aligned} \phi_{m-3} &= 1 - 7\zeta + 21\zeta^2 - 35\zeta^3 + 35\zeta^4 - 21\zeta^5 + 7\zeta^6 - \zeta^7, \\ \phi_{m-2} &= 120 - 392\zeta + 504\zeta^2 - 280\zeta^3 + 84\zeta^5 - 42\zeta^6 + 7\zeta^7, \\ \phi_{m-1} &= 1191 - 1715\zeta + 315\zeta^2 + 665\zeta^3 - 315\zeta^4 - 105\zeta^5 + 105\zeta^6 - 21\zeta^7, \\ \phi_m &= 2416 - 1680\zeta + 560\zeta^4 - 140\zeta^6 + 35\zeta^7, \\ \phi_{m+1} &= 1191 + 1715\zeta + 315\zeta^2 - 665\zeta^3 - 315\zeta^4 + 105\zeta^5 + 105\zeta^6 - 35\zeta^7, \\ \phi_{m+2} &= 120 + 392\zeta + 504\zeta^2 + 280\zeta^3 - 84\zeta^5 - 42\zeta^6 - 21\zeta^7, \\ \phi_{m+3} &= 1 + 7\zeta + 21\zeta^2 + 35\zeta^3 + 35\zeta^4 + 21\zeta^5 + 7\zeta^6 - 7\zeta^7, \\ \phi_{m+4} &= \zeta^7. \end{aligned} \quad (33)$$

By utilizing *Equations* (32) and (33), the following expressions are procured:

$$\begin{aligned} u'_m &= \frac{7}{h} (-\sigma_{m-3} - 56\sigma_{m-2} - 245\sigma_{m+1} + 245\sigma_{m+1} + 56\sigma_{m+2} + \sigma_{m+3}), \\ u''_m &= \frac{42}{h^2} (\sigma_{m-3} + 24\sigma_{m-2} + 15\sigma_{m-1} - 80\sigma_m + 15\sigma_{m+1} + 24\sigma_{m+2} + \sigma_{m+3}), \\ u'''_m &= \frac{210}{h^3} (-\sigma_{m-3} - 8\sigma_{m-2} + 19\sigma_{m-1} - 19\sigma_{m+1} + 8\sigma_{m+2} + \sigma_{m+3}), \quad u^{iv}_m = \\ &= \frac{840}{h^4} (\sigma_{m-3} - 9\sigma_{m-1} + 16\sigma_m - 9\sigma_{m+1} + \sigma_{m+3}), \\ u^v_m &= \frac{2520}{h^5} (-\sigma_{m-3} + 4\sigma_{m-2} - 5\sigma_{m-1} + 5\sigma_{m+1} - 4\sigma_{m+2} + \sigma_{m+3}). \end{aligned} \quad (34)$$

When, writing (32) and (33) in Equation (1) and making some simplification, the following systems of ODEs are achieved [64]:

$$\begin{aligned} &\dot{\sigma}_{m-3} + 120\dot{\sigma}_{m-2} + 1191\dot{\sigma}_{m-1} + 2416\dot{\sigma}_m + 1191\dot{\sigma}_{m+1} + 120\dot{\sigma}_{m+2} + \dot{\sigma}_{m+3} \\ &+ 45(Z_{m1} + 15Z_{m2}) \frac{7}{h} (-\sigma_{m-3} - 56\sigma_{m-2} - 245\sigma_{m+1} + 245\sigma_{m+1} + 56\sigma_{m+2} + \sigma_{m+3}) \\ &+ 15Z_{m3} \frac{210}{h^3} (-\sigma_{m-3} - 8\sigma_{m-2} + 19\sigma_{m-1} - 19\sigma_{m+1} + 8\sigma_{m+2} + \sigma_{m+3}) \\ &+ \frac{2520}{h^5} (-\sigma_{m-3} + 4\sigma_{m-2} - 5\sigma_{m-1} + 5\sigma_{m+1} - 4\sigma_{m+2} + \sigma_{m+3}) = 0, \end{aligned} \quad (35)$$

where $\dot{\sigma} = \frac{d\sigma}{dt}$ and

$$Z_{m1} = u^2 = (\sigma_{m-3} + 120\sigma_{m-2} + 1191\sigma_{m-1} + 2416\sigma_m + 1191\sigma_{m+1} + 120\sigma_{m+2} + \sigma_{m+3})^2,$$

$$Z_{m2} = u_{xx} = \frac{42}{h^2} (\sigma_{m-3} + 24\sigma_{m-2} + 15\sigma_{m-1} - 80\sigma_m + 15\sigma_{m+1} + 24\sigma_{m+2} + \sigma_{m+3}),$$

$$Z_{m3} = u = \sigma_{m-3} + 120\sigma_{m-2} + 1191\sigma_{m-1} + 2416\sigma_m + 1191\sigma_{m+1} + 120\sigma_{m+2} + \sigma_{m+3}.$$

In Equation (35), replacing $\dot{\sigma}_i$ by forward difference approximation $\dot{\sigma}_i = \frac{\sigma_i^{n+1} - \sigma_i^n}{\Delta t}$ and σ_i by Crank–Nicolson formulation $\sigma_i = \frac{\sigma_i^{n+1} + \sigma_i^n}{2}$ then the system of ODEs (35) turns into the following system

$$\lambda_1 \sigma_{m-3}^{n+1} + \lambda_2 \sigma_{m-2}^{n+1} + \lambda_3 \sigma_{m-1}^{n+1} + \lambda_4 \sigma_m^{n+1} + \lambda_5 \sigma_{m+1}^{n+1} + \lambda_6 \sigma_{m+2}^{n+1} + \lambda_7 \sigma_{m+3}^{n+1} = \lambda_7 \sigma_{m-3}^n + \lambda_6 \sigma_{m-2}^n + \lambda_5 \sigma_{m-1}^n + \lambda_4 \sigma_m^n + \lambda_3 \sigma_{m+1}^n + \lambda_2 \sigma_{m+2}^n + \lambda_1 \sigma_{m+3}^n, \quad (36)$$

where

$$\begin{aligned} \lambda_1 &= [1 - A - B - C], \\ \lambda_2 &= [120 - 56A - 8B + 4C], \\ \lambda_3 &= [1191 - 245A - 19B - 5C], \\ \lambda_4 &= [2416], \\ \lambda_5 &= [1191 + 245A - 19B + 5C], \\ \lambda_6 &= [120 + 56A + 8B - 4C], \\ \lambda_7 &= [1 + A + B + C], \\ A &= \frac{a}{2} \Delta t, B = \frac{b}{2} \Delta t, C = \frac{c}{2} \Delta t, \\ a &= \left[\frac{7k}{h} + \lambda Z_{m1} - \alpha Z_{m2} \right], \\ b &= \left[\frac{210}{h^3} \mu \right], \\ c &= \left[\frac{2520}{h^5} \beta \right]. \end{aligned} \quad (37)$$

By removing $\sigma_{-3}, \sigma_{-2}, \sigma_{-1}, \sigma_{N+2}$ and σ_{N+3} from the system (36), we get the following system

$$Rd^{n+1} = Sd^n \quad (38)$$

which can be solved at any desired time level by starting with the initial vector d^0 .

7. STABILITY ANALYSIS

The Von-Neumann stability analysis based on Fourier method has been implemented to examine the stability. Considering the following Fourier mode [65,66]:

$$\sigma_m^n = \xi^n e^{imkh} \quad (39)$$

into the iterative system (36) and after some amplifications,

$$\xi = \frac{p_1 - ip_2}{p_1 + ip_2}, \quad (40)$$

is obtained and in which

$$\begin{aligned} p_1 &= 2 \cos(3kh) + 240 \cos(2kh) + 2382 \cos(kh) + 2416, \\ p_2 &= (2A + 2B + 2C) \sin(3kh) + (112A + 16B - 8C) \sin(2kh) + \\ &\quad (490A - 38B + 10C) \sin(kh). \end{aligned} \quad (41)$$

The linearized scheme's stability is confirmed by the observation that $|\xi| = 1$, which is the highest value of (36).

8. RESULTS AND DISCUSSIONS

In this section, examples are ensured to demonstrate the robustness and productivity of the proposed numerical scheme. For a nonlinear initial and boundary value problem having an exact solution, the error norms L_2 and L_∞ described as [67,68]:

$$L_2 = \|u^{exact} - u_N\|_2 \simeq \sqrt{h \sum_{j=1}^N |u_j^{exact} - (u_N)_j|^2}, \quad (42)$$

$$L_\infty = \|u^{exact} - u_N\|_\infty \simeq \max_j |u_j^{exact} - (u_N)_j|, j = 1, 2, \dots, N \quad (43)$$

are generally used to test and evaluate the differences between exact and approximate solutions.

8.1. TEST PROBLEM 1

For this problem, Equation (1) has been handled for the parameters $\alpha = 4$, $\gamma = -3$ and $\beta = 1$ which gives:

$$u_t + 4uu_x - 3u^2u_x + u_{xxx} = 0. \quad (44)$$

Exact solution of the Gardner equation is

$$u(x, t) = \frac{2}{12 + 3\sqrt{14}\cosh\left[\frac{-x+5}{3} + \frac{t}{27}\right]} \quad (45)$$

which depicts a single solitary wave. To demonstrate precision of numerical scheme, the equation is investigated over the domain $[x_L = -20, x_R = 30]$ until time $t = 5$. In numerical experiments, $\Delta t = 0.1$; 0.01 with $h = 5$ and $h = 10$ have been taken in accordance with the references to be compared. Table (1) provides a full description of the corresponding findings, and the solutions mentioned therein have been compared to those found in the corpus of recent research. The table unequivocally demonstrates that our performance is satisfactory in comparison to studies from the literature Ref.[69], and the numerical results nearly reflect the exact solutions. Fig. 6 depicts the twodimensional instance of the descending bell-shaped wave solution as well as the contour line for the motion of each individual wave.

Table 1. Error norms for test problem 1.

	$\Delta t = 0.1, h = 10$		$\Delta t = 0.01, h = 10$	
t	L_2	L_∞	L_2	L_∞
1	1.3977E-04	3.6634E-05	6.0432E-04	1.8946E-04
2	2.7384E-04	7.2582E-05	1.1513E-03	3.6085E-04
3	4.0706E-04	1.0784E-04	1.6457E-03	5.1532E-04
4	5.3883E-04	1.4244E-04	2.0909E-03	6.5397E-04
5	6.6903E-04	1.7637E-04	2.4902E-03	7.7782E-04
[69] $t = 5$	-	1.9992E-03	-	1.9992E-03

	$\Delta t = 0.1, h = 10$		$\Delta t = 0.01, h = 10$	
	L_2	L_∞	L_2	L_∞
1	3.3085E-04	9.8974E-05	3.3151E-04	9.8868E-05
2	6.6056E-04	2.0175E-04	6.6320E-04	2.0116E-04
3	9.8976E-04	3.0793E-04	9.9655E-04	3.0623E-04
4	1.3179E-03	4.1708E-04	1.3319E-03	4.1337E-03
5	1.6447E-03	5.2871E-04	1.6701E-03	5.2180E-03

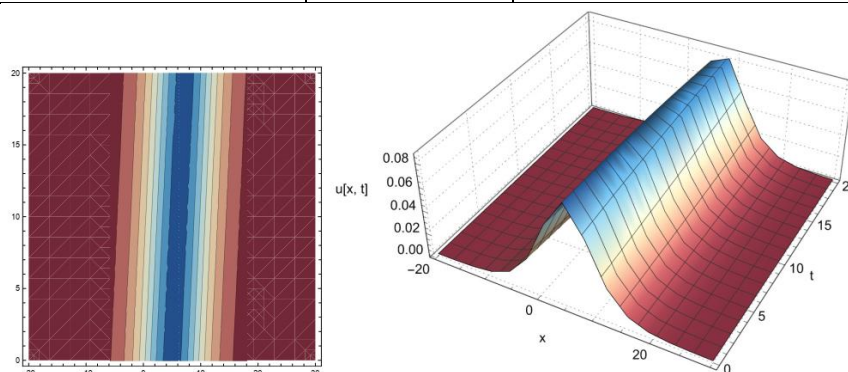


Figure 6. Single solitary wave and its contour line for test problem 1.

8.2. TEST PROBLEM 2

For this test problem, Equation (1) has been handled for the parameters $\alpha = 1$, $\gamma = -5$ and $\beta = 1$ which gives:

$$u_t + uu_x - 5u^2u_x + u_{xxx} = 0. \quad (46)$$

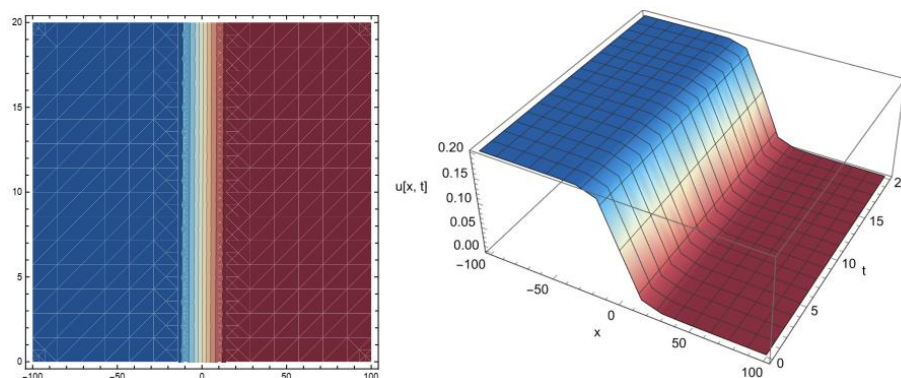
Using this approach, we model the second form of the Gardner equation, which yields folding type soliton solutions. The boundary conditions for the wave at infinity differ topologically from those in space because the twist solution is topological. These folded solitons are typically characterized by their persistent profile; that is, they are independent of time. A good real-world example of the buckling solution is the Bloch wall between two magnetic fields in a ferromagnet. Second form of the Gardner equation's exact solution is

$$u(x, t) = \frac{1}{10} \left(1 - \tanh \left(\frac{\sqrt{30}}{60} \left(x - \frac{t}{30} \right) \right) \right), \quad (47)$$

which corresponds to the motion of a single solitary wave. To show certainty of numerical algorithm, the equation is examined over the region $[x_L = -80, x_R = 80]$ until time $t = 1$. In numerical computations, $\Delta t = 0.1; 0.01$ with $h = 10$ and $h = 5$ have been selected in accordance with the references to be compared. Table (2) provides a full description of the corresponding findings, and the solutions mentioned therein have been compared to those found in the corpus of recent research. The table unequivocally demonstrates that our performance is satisfactory in comparison to studies from the literature Ref.[69], and the numerical results nearly reflect the exact solutions. Fig 7 displays simulations of a single soliton and the contour line for the motion of a single wave.

Table 2. Error norms for test problem 2.

	$\Delta t = 0.1, h = 10$		$\Delta t = 0.01, h = 10$	
t	L_2	L_∞	L_2	L_∞
0.1	1.2170E-05	3.6588E-06	1.2273E-04	3.8794E-05
0.2	2.4336E-05	7.3162E-06	2.4498E-04	7.7435E-05
0.3	3.6502E-05	1.0973E-05	3.6677E-04	1.1592E-04
0.4	4.8672E-05	1.4632E-05	4.8808E-04	1.5427E-04
0.5	6.0832E-05	1.8288E-05	6.0894E-04	1.9247E-04
[69] $t = 1$	-	2.9575E-04	-	2.9575E-04
	$\Delta t = 0.1, h = 5$		$\Delta t = 0.01, h = 5$	
t	L_2	L_∞	L_2	L_∞
0.1	6.3601E-06	2.0608E-06	.0008434571	3.7669E-05
0.2	1.2725E-05	4.1249E-06	.0016852925	7.5265E-05
0.3	1.9096E-05	6.1918E-06	.0025254961	1.1278E-04
0.4	2.5477E-05	8.2648E-06	.0033639561	1.5022E-04
0.5	3.1866E-05	10.3422E-06	.0042006541	1.8758E-04
1	6.3895E-05	20.0776E-06	.0083567125	3.7306E-04

**Figure 7. Single solitary wave and its contour line for test problem 2.**

9. CONCLUSIONS

The implications of our research are twofold. Firstly, we generate (G'/G) -expansion method for obtaining the exact solutions of the Gardner equation. The method is a standard and suitable for programming, which permits us to solve complex and complicate algebraic calculation. Secondly, the collocation method is presented and implemented for the numerical solution of the Gardner equation. The von Neumann method has been carefully applied to test the numerical algorithm's stability, and it has been shown to be unconditionally stable. The reliability and efficiency of the method have been evaluated using L_2 and L_∞ error norms, and the calculated results are seen to be better and more compatible than the results in the literature. Additionally, the solutions' behavior is visually depicted, demonstrating the similarities between the simulation of solutions over time and the numerical and exact solutions. The best part of the study is successful implementation of both the schemes for finding both exact and numerical results. From this, our methods are valid techniques for solving the Gardner equation, which can also be successfully used to solve a number of physically significant non-linear issues.

REFERENCES

- [1] Hollowa, P.E.P., Pelinovsky, E., Talipova, T., Barnes, B., *Journal of Physical Oceanography*, **27**, 871, 1997.
- [2] Gear, J. A., Grimshaw, R., *Physics of Fluids*, **26**, 14, 1989.
- [3] Watanabe, S., *Journal of the Physical Society of Japan*, **53**, 950, 1984.
- [4] Logan, J. D., *An Introduction to Nonlinear Differential Equations*, John Wiley and Sons, New York, United States, pp. 1-395, 2008.
- [5] Kadomtsev, B. B., Petviashvili, V. I., *Soviet Physics Doklady*, **192**(4), 539, 1970.
- [6] Zhang, H., *Applied Mathematics and Computation*, **216**(9), 2771, 2010.
- [7] Hu, W. Q., Gao, Y. T., Lan, Z. Z., Su, C. Q., Feng, Y. J., *Applied Mathematical Modelling*, **46**, 126, 2017.
- [8] Hirota, R., *Physical Review Letters*, **27**(18), 1192, 1971.
- [9] Ma, W. X., Zhang, Y., Tang Y., Tu, J., *Applied Mathematics and Computation*, **218**(13), 7174, 2012.
- [10] Vakhnenko, V. O., Parkes, E. J., Morrison, A. J., *Chaos, Solitons and Fractals*, **17**(4), 683, 2003.
- [11] Barman, H. K., Roy, R., Mahmud, F., Akbar M. A., Osman, M. S., *Optik*, **17**(4), 166294, 2021.
- [12] Rezazadeh, H., Ullah, N., Akinyeni, L., Shah, A., Alzamin, S. M. M., Chu, Y. M., Ahmad, H., *Results in Physics*, **24**, 104179, 2021.
- [13] Khater, M. M. A., Elagen, S. K., Mousa, A. A., Shorbagy, A. A. E., Alfalqi, S. H., Alzaidi, J. F., Lu, D., *Results in Physics*, **25**, 104133, 2021.
- [14] Baskonus, H. M., *An International Journal of Optimization and Control: Theories and Applications*, **11**(1), 92, 2021.
- [15] Ablowitz, M. J., Clarkson, P. A., *Solitons, Nonlinear Evolution Equations and Inverse Scattering*, New York, NY, Cambridge University Press, 1991.
- [16] Xu, L. P. and Zhang, J. L., *Chaos Solitons Fractals*, **31**, 937, 2007.
- [17] Wazwaz, A. M., *Communications in Nonlinear Science and Numerical Simulation*, **12**, 904, 2007.
- [18] He, J. H., Wu, X. H., *Chaos Solitons and Fractals*, **30**, 700, 2006.
- [19] Akbar, M. A., Ali, N. H. M., *World Applied Sciences Journal*, **17**(12), 1603, 2012.
- [20] Wang, M. L., Li, X. Z., Zhang, J., *Physics Letters A*, **372**, 417, 2008.
- [21] Taghizade, N., Neirameh, A., *International Journal of Nonlinear Sciences and Numerical Simulation*, **9**(3), 305, 2010.
- [22] Zhang, S., Tong, J., Wang, W., *Physics Letters A*, **372**, 2254, 2008.
- [23] Akbar, M. A., Ali, N. H. M., Zayed, E. M. E., *Mathematical Problems in Engineering*, **2012**, 1, 2012.
- [24] Zayed, E. M. E., Zedan, H. A., Gepreel, K. A., *Chaos Solitons and Fractals*, **22**, 285, 2004.
- [25] Chen, Y., Wang, Q., *Chaos Solitons and Fractals*, **24**, 745, 2005.
- [26] Secer, A., *An International Journal of Optimization and Control: Theories and Applications*, **8**(2), 250, 2018.
- [27] Hirota, R., *Direct Methods in Soliton Theory*. In: Bullough, R.K., Caudrey, P.J. (Eds). *Solitons*, Springer, Berlin, 1980.
- [28] Qin, Z. Y., *Journal of the Physical Society of Japan*, **76**, 124004, 2007.
- [29] Kocak, H., *An International Journal of Optimization and Control: Theories and Applications*, **11**(2), 123, 2021.

- [30] Miura, R. M., Gardner, C. S., Kruskal, M. D., *Journal of Mathematical Physics*, **9**, 1204, 1968.
- [31] Degon, L., Chowdhury, A., *Partial Differential Equations in Applied Mathematics*, **5**, 100310, 2022.
- [32] Kamchatnov, A. M., Kuo, Y. H., Lin, T. C., Horng, T. L., Gou, S. C., Clift, R., Grimshaw, R. H. J., *Physical Review E*, **86**, 036605, 2012.
- [33] <http://dx.doi.org/10.1103/PhysRevE.86.036605>
- [34] Grimshaw, R., *Environmental Stratified Flows*, Springer Science and Business Media, Berlin, Germany pp. VIII-284, 2002.
- [35] Helfrich, K. R., Melville, W. K., *Annual Review of Fluid Mechanics*, **38**(1), 395, 2006.
- [36] Ruderman, M., Talipova, T., Pelinovsky, E., *Journals Journal of Plasma Physics*, **74**, 639, 2008.
- [37] Vosconcelos, G. L., Kaclanoff, L. P., *Physical Review Journals A*, **44**, 6490, 1991.
- [38] Malfliet, W., Hereman, W., *Physica Scripta*, **54**, 563, 1996.
- [39] Malfliet, W., Hereman, W., *Physica Scripta*, **54**, 569, 1996.
- [40] Kaya, D., Inan, I. E., *Applied Mathematics and Computation*, **168**, 915, 2005.
- [41] Dinarvand, S., Khosravi, S., Khoosheh, H., Nasrollahzadeh, M., *Mathematical Methods in the Applied Sciences*, **21**, 1037, 2011.
- [42] Krishnan, E., Triki, H., Labidi, M., *Nonlinear Dynamics*, **66**, 497, 2011.
- [43] Li, W., Ma, X., *Mathematical Methods in the Applied Sciences*, **5**(73), 3607, 2011.
- [44] Gomes, J. F., Franca, G. S., Zimmerman, A. H., *Journal of Physics A*, **45**, 1527, 2011.
- [45] Biswas, A., *Advanced Studies in Theoretical Physics*, **2**, 787, 2008.
- [46] Taghizade, N., Neirameh, A., *International Journal of Nonlinear Sciences and Numerical Simulation*, **9**, 305, 2010.
- [47] Gardner, G. H. F., Gardner, L. W., Gregory, A. R., *Geophysics*, **39**(6), 770, 1974.
- [48] Sluynyaev, A. V., *Journal of Experimental and Theoretical Physics*, **92**, 529, 2001.
- [49] Slyunyaev, A., Pelinovsky, E., *Journal of Experimental and Theoretical Physics*, **89**, 173, 1999.
- [50] Miles, J. W., *Tellus*, **33**, 397, 1981.
- [51] Wadati, M., *Journal of the Physical Society of Japan*, **38**, 673, 1975.
- [52] Wadati, M., *Journal of the Physical Society of Japan*, **38**, 681, 1975.
- [53] Coffey, M. W., *SIAM Journal on Applied Mathematics*, **50**(6), 1580, 1990.
- [54] Mohamad, M. N. B., *Mathematical Methods in the Applied Sciences*, **15**(2), 73, 1992.
- [55] Lou, S., *Mathematical Methods in the Applied Sciences*, **17**(5), 339, 1994.
- [56] Zhang, J., *Int. J. Theor. Phys.*, **37**(5), 1541, 1998.
- [57] Wazwaz, A.M., *Communications in Nonlinear Science and Numerical Simulation*, **12**, 1395, 2007.
- [58] Nishiyama, H., Noi, T., *Computational and Applied Mathematics*, **35**, 75, 2016.
- [59] Rageh, T. M., Salem, G., El-Salam, F. A., *International Journal of Advances in Applied Mathematics and Mechanics*, **1**, 1, 2014.
- [60] Tiong, W. K., Tay, K. G., Ong, C. T., Sze, S. N., *Proceedings of the International Conference on Computing. In: Mathematics and Statistics*, 243, 2017.
- [61] Shallal, M., Ali, K. K., Raslan, K. R., Rezazadeh, B. A., *Journal of Ocean Engineering and Science*, **5**, 323, 2020.
- [62] Prenter, P. M., *Splines and Variational Methods*, Wiley-interscience Publication, New York, 1975.
- [63] Baker, C. T. H., *Clarendon Press, Oxford*, 296, 1976.
- [64] Ali, K. K., Sucu, D. Y., Karakoc, S. B. G., *Mathematics and Computers in Simulation*, **220**, 192, 2024.
- [65] Karakoc, S. B. G. Saha, A., Bhowmik, S. K., Sucu, D. Y., *Wave Motion*, **181**, 103, 2023.

- [66] Yagmurlu, M., Ucar, Y., Bashan A., *Adiyaman University Journal of Science*, **9**(2), 386, 2019.
- [67] Kutluay, S., Yagmurlu, M., Karakaş, A. S., *International Journal of Mathematics and Computer in Engineering*, **3**(2), 253, 2025.
- [68] Karakoc, S. B. G., Sucu, D. Y., Taghachi, M. A., *Journal of Universal Mathematics*, **5**(2), 108, 2022.
- [69] Yagmurlu, M., Karakaş, A. S., *Computational Methods for Differential Equations*, **10**(4), 1046, 2022.
- [70] Degon, L., Chowdhury, A., *Partial Differential Equations in Applied Mathematics*, **5**, 100310, 2022.